

Cite this: DOI: 10.1039/c0cp02936j

www.rsc.org/pccp

## Bottom-up computational modeling of semi-crystalline fibers: from atomistic to continuum scale

Murat Cetinkaya,<sup>a</sup> Senbo Xiao<sup>b</sup> and Frauke Gräter<sup>\*b</sup>

Received 21st December 2010, Accepted 28th March 2011

DOI: 10.1039/c0cp02936j

**A bottom-up computational approach involving Molecular Dynamics (MD) of silk fiber subunits and Finite Element (FE) simulations of whole spider silk fibers is presented. The approach is discussed with an emphasis on the benefits and bottlenecks of incorporating the atomistic and continuum models of crystalline and disordered domains in the fibers. The approach does not require any empirical parameters and it is applicable to similar semi-crystalline systems.**

Semi-crystalline fibers such as spider and silkworm silk are natural materials with intriguing mechanical properties. Being composed of stiff crystalline and soft disordered domains (Fig. 1a), these fibers combine elasticity, strength, and toughness in a tailored manner through a variation in the chemistry (e.g. amino acid composition),<sup>1–3</sup> architecture (e.g. domain size),<sup>4</sup> and ambient conditions (e.g. humidity).<sup>5</sup> Although such advanced materials show a big potential in engineering applications, the production of these natural fibers in industrial quantities is a challenging process. On the other hand, artificial fibers mostly show a poorer mechanical performance compared to their natural counterparts.<sup>1</sup> Therefore, it is critical to have a thorough understanding of the natural semi-crystalline fibers, in particular the relationship between their structural and mechanical properties.

Experimental studies regarding silkworm and spider silk fibers have provided detailed insight to the material chemistry and macroscopic mechanical properties.<sup>1–8</sup> However, the precise structural architecture that originates from molecular ordering and, correspondingly, the mechanics at the atomistic level are some of the points lacking a general agreement. Due to technical difficulties in experimental studies, computational methods have become a feasible alternative when investigating individual silk fiber domains at the atomistic scale.<sup>9–12</sup> Nevertheless, the gap between atomistic and higher length scales needs to be properly addressed if one aims to establish an understanding between the structural ordering at the molecular level and the mechanical properties at the macroscopic level.

Here, we focus on the methodological aspects of our bottom-up approach by addressing three major questions of incorporating the parameters of atomistic scale simulations into a mesoscopic model for silk fiber mechanics. Our bottom-up approach is based on subjecting all-atom models of the representative silk fiber domains to a pulling force in order to determine their mechanical properties at the nanoscale. First, we will discuss a major point of concern at this stage, the pulling speed and the pulling setup used for the crystalline domains in MD simulations. The disordered domains of silk fibers show pronounced differences from simple polymer models for single chains due to their specific coiling behavior and additional entanglement effects, which we will quantify in the second part. Thirdly, we will focus on the final step of our approach, namely building a comprehensive fiber model with a correct treatment of its two major constituents, *i.e.* the crystalline and disordered domains.

One needs to determine the elastic and rupture parameters of the highly ordered,  $\beta$ -strand rich, silk crystalline domains for their continuum scale models. Our bottom-up approach includes Force-Probe MD simulations in which the crystals are subjected to a pulling force mimicking the mechanical load acting on them as in a macroscopic fiber. When compared to the experimental values, the loading rates in Force-Probe MD simulations are typically several orders of magnitude higher. To quantify the effect of the loading rate on the force-extension behavior, we have covered a range of pulling speeds (0.05–0.20 m/s) with a range of spring constants (0.83–8.3 N/m), thereby achieving up to 1 : 40 loading rates. We observed that, within this range, the crystal rupture force (and similarly, the rupture stress) vary by  $\sim 11\%$  (Fig. 1b).<sup>10</sup> However, this increase in rupture force with loading rate translates to only a minor increase in crystal toughness of  $\sim 5\%$ . This is due to the negligible increase in strain right before rupture, where the force-extension curve shows pronounced stiffening. Notwithstanding, we conclude that our estimates of rupture stresses and toughness represent the upper limits due to the limited time scale of the all-atom simulations.

Another issue we here address is the pulling setup in MD and FE simulations. Compared to similar studies involving spider silk crystals,<sup>11</sup> the boundary conditions in our MD simulations are not restricted. Even in the absence of any constraints and being independent of the way the force is applied, the silk fiber domains stay intact until the rupture

<sup>a</sup> BASF SE, Carl-Bosch Strasse 38, Ludwigshafen 67056, Germany.  
E-mail: murat.cetinkaya@basf.com

<sup>b</sup> Heidelberg Institute for Theoretical Studies,  
Schloss-Wolfsbrunnengasse 35, Heidelberg 69118, Germany.  
E-mail: senbo.xiao@h-its.org, frauke.graeter@h-its.org;  
Fax: +49 6221 533298; Tel: +49 6221 533267

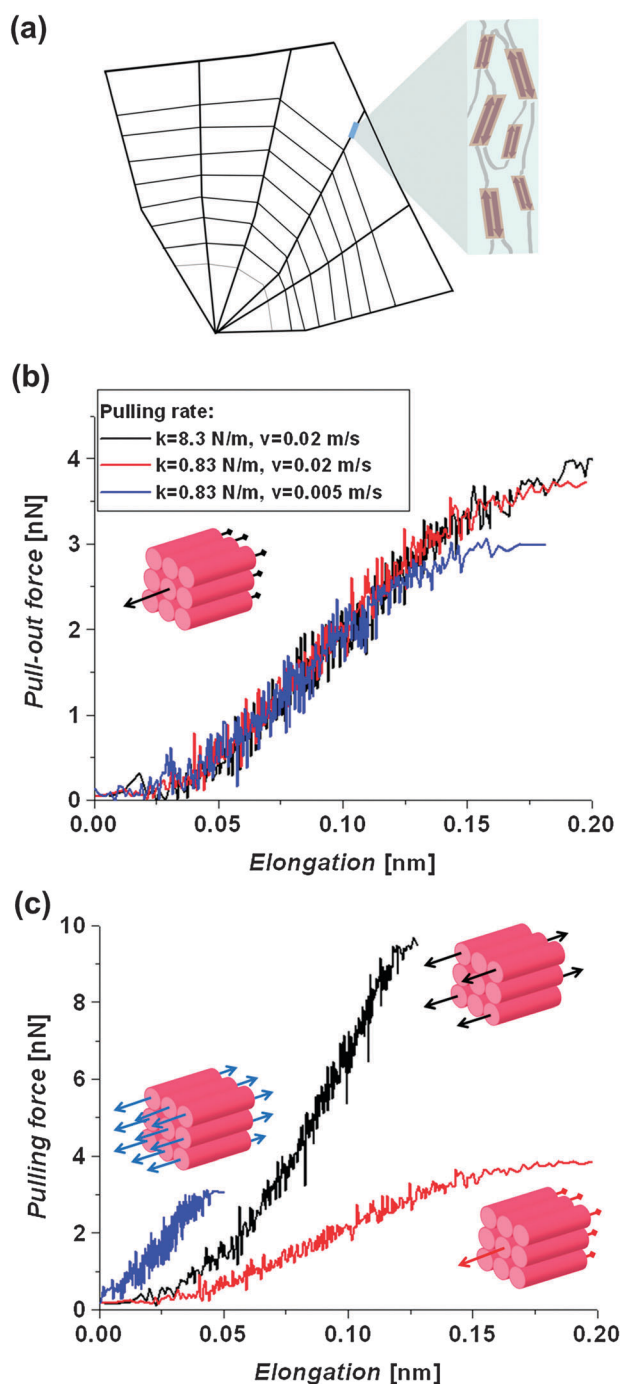


**Fig. 1** Spider silk fibers and the mechanical behavior of the crystalline domains under different conditions of loading. (a) The schematic of spider silk radial thread being composed of crystalline domains cross linking disordered chains. The mechanical behavior of the crystalline domains may vary with different loading rates (b), and loading setups (c). Schematics in (b) and (c) show the pulling setups in MD simulations. Blue curve in (c) ends not due to rupture, but the simulation time. The silk crystals have a size of  $\sim 3 \times 2.5 \times 2.5 \text{ nm}^3$ .

point in MD simulations, which is the hallmark behavior of a brittle material. This observation highlights the role of non-bonded interactions between the  $\beta$ -strands in silk crystals. They cooperatively dissociate at the rupture event of the crystal, giving rise to nanoNewton scale forces.

The detailed arrangement and entanglement of the amorphous chains, and therefore the connectivity between crystals, are not known and likely to vary within and between fibers, as they depend among other factors during the spinning procedure. In Fig. 1c, we compare different loading schemes in silk crystals, which represent different scenarios for their connections to the amorphous phase. As expected, pulling all  $\beta$ -strands from both of their termini (blue curve in Fig. 1c), which represents the ideal case of high order in the fiber in the absence of chain entanglement, results in a higher stiffness and lower elongation when compared to the case where only one  $\beta$ -strand is pulled out of a crystal (red curve). In the former case, the load is dominantly axial, and it is mainly carried by the stiff backbone elements due to the homogeneous loading of all  $\beta$ -strands. The latter case might result from high disorder and thus heterogeneous loading in the amorphous matrix. Consequently, the load is primarily translated into shear forces from the pulled to the adjacent strands. Therefore, the load is mainly carried by the weaker hydrogen bonds and the side chain interactions between the  $\beta$ -strands. In natural silk fibers, depending on the entanglement of the disordered chains, a certain subset of  $\beta$ -strands within a crystal will be subjected to a pulling force along the fiber axis in opposite directions, resulting in a situation between these two extremes. In order to include both the axial and shear loading effects in our MD simulations, the  $\beta$ -strands are pulled from one terminus or the other in an alternating pattern (black curve). In this case, the crystalline domain showed, unsurprisingly, an intermediate stiffness. However, it exhibited an enormously strong mechanical behavior, with a rupture stress in the 10 nN range. In silk fibers, the heterogeneity in the loading of disordered chains that are connected to the silk crystals will vary with respect to the mechanical and thermal history of the fiber. The alternating pulling pattern (black curve), lying in between the two other extremes, represents an intermediate heterogeneity in the loading of disordered chains connected to the silk crystal. It can be considered an average scenario, and hence as the method of choice for parameterization of the continuum scale model.

The disordered domains of the silk fibers are semi-extended peptide chains mainly composed of glycine.<sup>1</sup> The force-extension curve of such a chain has been obtained from umbrella sampling MD simulations.<sup>10</sup> Such a force-extension curve implicitly reflects the extent of non-bonded interactions, such as hydrogen bonds, causing the peptide to coil. At extensions up to 8 nm, the mechanical behavior of an individual chain resembles a worm-like chain (WLC),<sup>13</sup> with a non-linear, neo-Hookean like elastic behavior. However, at higher extensions, the WLC model overestimates the coiling propensity. Due to this complex elastic behavior, the complete transfer of the force-extension curve of a peptide chain was chosen instead of using an analytic WLC type expression in a multiscale approach (Fig. 2a).<sup>10</sup> Therefore, in FE simulations a disordered peptide chain was represented by a non-linear elastic member with its stiffness calculated from the input force-extension curve.

To dissect the contributions of the crystalline and disordered domains when they are combined as in a silk fiber, we have probed the mechanics of a composite unit that is composed of crystalline and disordered domains coupled in a serial fashion. The all-atom composite unit subjected to a pulling force in

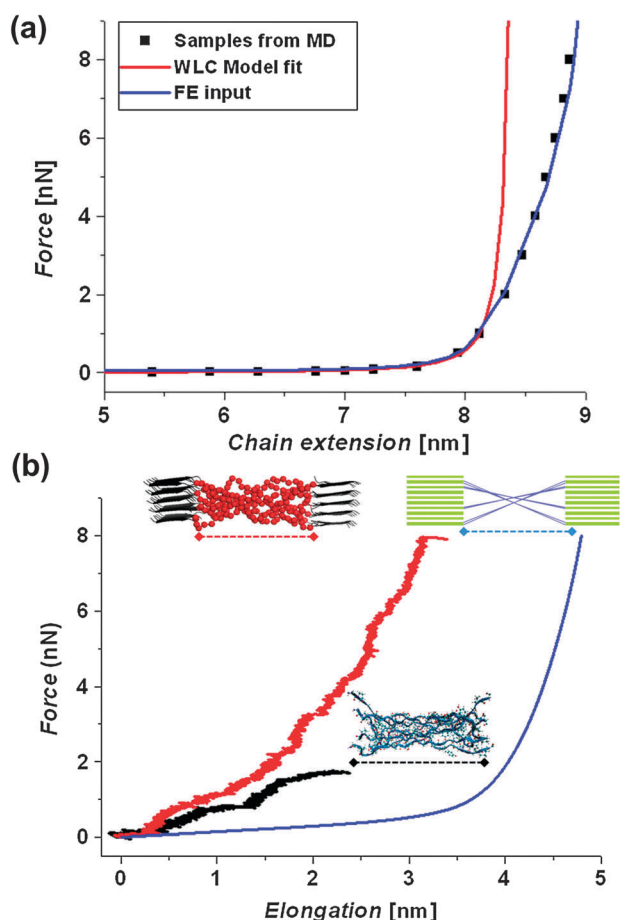


**Fig. 2** The mechanical behavior of disordered peptides in silk fibers. (a) Force-extension data of a single peptide from umbrella sampling MD simulations (black) and the WLC model fit between 4.50 and 8.49 nm chain extension (red curve, persistence length: 0.54 nm, contour length: 8.49 nm). The input for the skeleton model is shown with the blue curve. (b) Force-elongation curves of a disordered domain coupled to crystalline domains (red: all-atom, blue: skeleton) and without any cross-linking (black: all-atom).

Force-Probe MD simulations shows a non-linear elastic behavior with stiffening at high extensions prior to rupture (Fig. 2b). We can derive the elastic moduli of crystalline and disordered domains as 80.0 GPa and 2.7 GPa, respectively.<sup>10</sup> While the force-extension curve shown in Fig. 2a accurately represents the behavior of a single chain, multiple entangled chains as present in the composite unit show a stiffer behavior when compared to an assembly of individual chains (Fig. 2b).<sup>10</sup> The extension of disordered domain involves the friction between the entangled chains. This increases the mechanical work the disordered domain can take up, when compared to a scenario where the individual chains do not interact with each other. The amino acid sequence of spider silk implies that the repeated crystalline domains act as cross-linking sites between these disordered chains. Consequently, these chains combine high elasticity and toughness when the silk fiber is extended up to its toughness limit. On the other hand, in the absence of cross-linking silk crystals, the peptide chains in the disordered domains disengage easily, with a much lower rupture force (2 nN as compared to 8 nN, Fig. 2b).

Then, a simplified FE model was constructed for FE analysis. The model consists of silk crystals built with elastic members representing the covalent bonds, side-chain packings, and hydrogen bonds and of members for disordered chains with an elasticity deduced from Fig. 2a.<sup>10</sup> Qualitatively, this skeleton model of the composite unit shows the same non-linear response to the applied pulling force. However, the all-atom model is stiffer due to the entanglement effects between the chains in the disordered domain (Fig. 2b). We note that the topology of the disordered domain, *i.e.* how the chains connect the crystalline domains, is based on an arbitrary choice of entanglement.

The all-atom model of the composite unit, given its size and complexity, does not allow to systematically scan other potential structural variables like crystallinity or entanglement. In fact, it features a crystallinity of  $\sim 68\%$ , which is much higher than those in natural silk fibers (10–25%). Hence, an interesting application of the skeleton model is to test various topologies which differ in the extent of entanglement and crystallinity, both of which are likely to be controlled by the degree of shear flow in the glands of the spider during fiber spinning.

In contrast to standard FE simulations, which are not capable of showing rupture properties, a major benefit of the all-atom model is the provided insight into the rupture mechanism of silk fibers. More specifically, the all-atom model shows that the failure in the composite unit originates from the disengagement of  $\beta$ -strands from the crystalline domains, emphasizing the role of crystalline units as force-bearing cross links.

The final step of our multiscale approach is to establish a comprehensive fiber model at the continuum scale. Similar to other computational studies regarding supramolecular peptide assemblies<sup>14</sup> and polymer/clay nanocomposites,<sup>15</sup> the spider silk fiber is modeled with a cylindrical solid member composed of a soft continuous phase representing the disordered domains, and strong rectangular phases for the crystalline domains. Disordered domains are represented with a linear elastic and isotropic material model, parameters of which are derived from all-atom simulations (Fig. 2b), thereby implicitly including non-covalent interactions along and within the chains. Based on the rupture observed in the composite unit (see above and Fig. 2b), we have established the definition of fiber rupture in the continuum model as the state in which the crystalline domains reach their rupture stress, which needs to be estimated from the corresponding all-atom models.<sup>10</sup> Hence, once the rupture stress of a crystalline domain is calculated, one can use it as an input in a higher scale model in order to estimate the fiber rupture. Treating the disordered domain as a linear-elastic continuum is a radical approximation. Incorporating a non-linear mechanical behavior that also takes the way of entanglement into account can be expected to strongly improve the accuracy of our calculations.

Crystalline domains, on the other hand, require a more precise treatment due to their highly ordered architecture. All-atom as well as simpler skeleton models of the silk crystals show a nonisotropic mechanical behavior, reflecting the specific arrangements of hydrogen bonds and side chain packings.<sup>10</sup> These rectangular blocks exhibit stronger mechanical characteristics along the backbone axis (which coincides with the fiber axis) and weaker, but similar properties in the transverse directions.

For instance, a  $2.5 \times 2 \times 2 \text{ nm}^3$  all-alanine spider silk crystal has 74.0 GPa longitudinal and 35.6 GPa transverse elastic moduli along with a shear modulus of 6.2 GPa on transverse plane. One could, therefore, approximate this mechanical behavior as one of a transversely isotropic material. Such an approximation renders the model to be less computationally demanding, but still maintains the essential characteristics of silk fibers as reported by compression tests.<sup>16</sup> Furthermore, the elastic and shear moduli of crystalline domains are geometry dependent (unpublished results). For this reason, the stiffness matrix of a crystal of a certain size needs to be calculated with the appropriate skeleton models, otherwise the results from the comprehensive fiber model would be misleading.

The comprehensive fiber model not only allows us to reach higher length and time scales with a tremendous decrease in computational cost ( $\sim 6$  orders of magnitude for a system which would comprise several million atoms), but also provides the opportunity of designing new fibers with varying structural architecture and crystallinity.<sup>10</sup> When compared to experimental results, our calculations indicate that the structural architecture of spider silk may be of serial or random type, where the crystalline domains are oriented in lamellar or scattered fashions with respect to the disordered domains, respectively. Furthermore, the comprehensive fiber model shows that the serial orientation of domains would lead to higher toughness properties, provided that the domains are precisely oriented at the nanoscale. The comprehensive model is able to predict the elastic mechanical properties of spider silk fibers, whereas it underestimates the rupture and toughness properties due to the FE simulations discarding the plastic deformation in disordered domains. Therefore, the rupture strain and toughness values from FE simulations are expected to be the lower boundaries of the actual values.

The bottom-up computational approach we present here combines two discrete simulation methods namely, MD and FE, while benefiting from the accuracy of the former and the speed of the latter method. All-atom models from MD simulations provide the initial geometry and structural parameters for the skeleton models, which are also dependent on the pulling speed and the pulling setup. The skeleton models in FE simulations allow a wider sampling range with lower computational cost. Compared to skeleton models, the all-atom models are capable of showing the rupture in small domains and other important mechanical behavior such as the stiffness of the entangled peptide chains. The comprehensive fiber model is based on the results from MD and FE simulations of small domains and allows us to investigate the essential parameters in artificial fiber design such as structural architecture

or crystallinity level. Proper treatment of the fiber constituents, e.g. transverse isotropy in crystalline domains, is of fundamental importance.

Compared to other studies in the literature, our models are not based on any empirical results and the utilized parameters and boundary conditions are not biased towards a desired material behavior. Our results from silk fiber models agree well with experiments, with regard to the elastic modulus, the rupture stress, and toughness.<sup>10</sup> The refinements of the approximations made during the upscaling might further improve the accuracy. Therefore, our method provides a framework for future studies regarding not only silk fibers, but also other semi-crystalline materials such as nacre and polyamides.

## Acknowledgements

This study was supported by a postdoctoral fellowship of the Alexander von Humboldt Foundation (to M.C.), the Klaus Tschira Foundation, the Chinese Academy of Sciences, and the Global Networks program at Heidelberg University as part of the Excellence Initiative.

## Notes and references

- 1 J. M. Gosline, P. A. Guerette, C. S. Ortlepp and K. N. Savage, *J. Experimental Biol.*, 1999, **202**, 3295.
- 2 K. N. Savage and J. M. Gosline, *J. Exp. Biol.*, 2008, **211**, 1937.
- 3 B. O. Swanson, T. A. Blackledge, J. Beltran and C. Y. Hayashi, *Appl. Phys. A: Mater. Sci. Process.*, 2005, **82**, 213.
- 4 N. Du, X. Y. Liu, J. Narayanan, L. Li, M. L. M. Lim and D. Li, *Biophys. J.*, 2006, **91**, 4528.
- 5 R. Ene, P. Papadopoulos and F. Kremer, *Soft Matter*, 2009, **5**, 4568.
- 6 F. Hagn, L. Eisoldt, J. G. Hardy, C. Vendrely, M. Coles, T. Scheibel and H. Kessler, *Nature*, 2010, **465**, 239.
- 7 N. Becker, E. Oroudjev, S. Mutz, J. P. Cleveland, P. K. Hansma, C. Y. Hayashi, D. E. Makarov and H. G. Hansma, *Nat. Mater.*, 2003, **2**, 278.
- 8 T. Lefevre, M. E. Rousseau and M. Pezolet, *Biophys. J.*, 2007, **92**, 2885.
- 9 S. Xiao, W. Stacklies, M. Cetinkaya, B. Markert and F. Graeter, *Biophys. J.*, 2009, **96**, 3997.
- 10 M. Cetinkaya, S. Xiao, B. Markert, W. Stacklies and F. Gräter, *Biophys. J.*, 2011, **100**, 1298–1305.
- 11 S. Keten, Z. Xu, B. Ihle and M. J. Buehler, *Nat. Mater.*, 2010, **9**, 359.
- 12 S. A. Fossey and S. Tripathy, *Int. J. Biol. Macromol.*, 1999, **24**, 119.
- 13 C. Bustamante, J. F. Marko, E. D. Siggia and S. Smith, *Science*, 1994, **265**, 1599.
- 14 X. Chen, Q. Cui, Y. Tang, J. Yoo and A. Yethiraj, *Biophys. J.*, 2008, **95**, 563.
- 15 D. Sikdar, S. M. Pradhan, D. R. Katti, K. S. Katti and B. Mohanty, *Langmuir*, 2008, **24**, 5599.
- 16 F. K. Ko and J. Jovicic, *Biomacromolecules*, 2004, **5**, 780.